Title
SUMO modification of cell surface Kv2.1 potassium channels regulates the activity of rat hippocampal neurons.

Journal
The Journal of general physiology, 137(5)

ISSN
0022-1295

Authors
Plant, Leigh D
Dowdell, Evan J
Dementieva, Irina S
et al.

Publication Date
2011-05-01

DOI
10.1085/jgp.201110604

SUMO modification of cell surface Kv2.1 potassium channels regulates the activity of rat hippocampal neurons

Leigh D. Plant, Evan J. Dowdell, Irina S. Dementieva, Jeremy D. Marks, and Steve A.N. Goldstein

Department of Pediatrics and Institute for Molecular Pediatric Sciences, Biological Sciences Division, Pritzker School of Medicine, University of Chicago, Chicago, IL 60637

Voltage-gated Kv2.1 potassium channels are important in the brain for determining activity-dependent excitability. Small ubiquitin-like modifier proteins (SUMOs) regulate function through reversible, enzyme-mediated conjugation to target lysine(s). Here, sumoylation of Kv2.1 in hippocampal neurons is shown to regulate firing by shifting the half-maximal activation voltage ($V_{1/2}$) of channels up to 35 mV. Native SUMO and Kv2.1 are shown to interact within and outside channel clusters at the neuronal surface. Studies of single, heterologously expressed Kv2.1 channels show that only K470 is sumoylated. The channels have four subunits, but no more than two non-adjacent subunits carry SUMO concurrently. SUMO on one site shifts $V_{1/2}$ by 15 mV, whereas sumoylation of two sites produces a full response. Thus, the SUMO pathway regulates neuronal excitability via Kv2.1 in a direct and graded manner.

The Journal of General Physiology

INTRODUCTION

Small ubiquitin-like modifier proteins (SUMOs) act via covalent linkage to the ε-amino group of specific lysine residues on target proteins. SUMOs and the enzymes that mature, activate, conjugate, and deconjugate are conserved from yeast to humans (Melchior et al., 2003). The majority of more than 70 recognized SUMO targets are transcription factors that operate in the nucleus. In this manner, SUMOs exert slow control over central nervous system excitability, for example, by management of synapse formation (Shalizi et al., 2006).

Previously, we demonstrated that the SUMO pathway can also act outside the nucleus on cell surface targets, for example, to regulate the operation of cloned K2P1 background potassium channels via direct modification (Rajan et al., 2005; Plant et al., 2010). Here, sumoylation and desumoylation are shown to alter the excitability of rat hippocampal neurons through reversible regulation of I_{DR}, a native potassium current passed by Kv2.1 channels.

First, the electrophysiological responses of hippocampal neurons in culture to intracellular application of wild-type and mutant SUMOs and Sentrin-specific protease (SENP)1 desumoylases were assessed. This demonstrated that sumoylation and desumoylation controlled neuronal excitability primarily via changes in the G-V relationship for I_{DR} activation. Next, sumoylation of native Kv2.1 channels by endogenous SUMO2/3 was observed by fluorescence resonance energy transfer (FRET) microscopy both within and outside characteristic Kv2.1 clusters in the soma and proximal dendrites. To identify the site(s), stoichiometry, orientation, and the graded impact of SUMO modification on Kv2.1, heterologously expressed channels were evaluated using live-cell FRET microscopy, single-molecule fluorimetry, electrophysiology, and mass spectrometry (MS).

The SUMO pathway is ubiquitous. Kv2.1 channels are expressed in the nervous system, heart, skeletal muscle, pulmonary arteries, and pancreas. Here, we demonstrate that sumoylation–desumoylation of surface Kv2.1 in hippocampal neurons alters the biophysical parameters of channel function, leading to modified cellular activity. This mechanism is expected to operate throughout the body.

MATERIALS AND METHODS

Cell culture, heterologous expression, and immunocytochemistry

Chinese hamster ovary (CHO) cells (American Type Culture Collection) were maintained in F12 media with 10% FBS and 1% penicillin and streptomycin. Plasmids were transfected into cells with Lipofectamine 2000 (Invitrogen). Experiments were performed 24–48 h after transfection at room temperature unless otherwise stated. Hippocampal neurons were prepared from E17

Correspondence to Steve A.N. Goldstein: sangoldstein@uchicago.edu

Abbreviations used in this paper: CFP, cyan fluorescent protein; CHO, Chinese hamster ovary; FRET, fluorescence resonance energy transfer; GFP, green fluorescent protein; MS, mass spectrometry; SAE, small ubiquitin-like modifier protein–activating enzyme; SENP, Sentrin-specific protease; SUMO, small ubiquitin-like modifier protein; TIRF, total internal reflection fluorescent; Ubc9, SUMO-conjugating enzyme; YFP, yellow fluorescent protein.

The Rockefeller University Press $30.00
J. Gen. Physiol. Vol. 137 No. 5 441–454
www.jgp.org/cgi/doi/10.1085/jgp.201110604

Sprague-Dawley rats as described previously (Marks et al., 2005), seeded to poly-L-lysine–coated glass coverslips, and maintained in Neurobasal medium with B27 supplement and Glutamax (Invitrogen) in a humidified atmosphere (5% CO_2 at 37°C). Immunostaining for the neuron-specific marker NeuN, as well as for oligodendrocyte- and astrocyte-specific markers, demonstrated that cultures were >98% neurons (not depicted).

For immunocytochemical studies, neurons were fixed with 4% paraformaldehyde, permeabilized with Triton X-100, and processed for immunostaining. Cells were incubated with validated antibodies to SUMO1 (1:250; ab32058; Abcam), SUMO2/3 (1:100; ab3742; Abcam), or GAPDH (1:250; ab37168; Abcam). For SUMO1 staining, cells were first incubated in 30 mM Tris-HCl, pH 7.4, at 95°C for 20 min. Binding was detected with Alexa Fluor 594–labeled, highly cross-adsorbed goat anti–rabbit IgG (1:500; Invitrogen). Kv2.1 was identified with a monoclonal antibody (1:5,000; NeuromAb), and binding was detected with Alexa Fluor 488–labeled, highly cross-adsorbed goat anti–mouse IgG (1:500; Invitrogen). To assess cross-reactivity of the anti–rabbit secondary antibody, identical labeling experiments were performed in the absence of the primary antibody. Cells were incubated in DAPI (300 nM for 3 min) and mounted in SlowFade (Invitrogen).

For colocalization studies, stained neurons were imaged with a 100× NA 1.45 oil objective on a laser-scanning confocal microscope (SP5; Leica) with identical illumination acquisition settings. Sequential images of Alexa Fluor 488 and Alexa Fluor 594 were obtained using laser lines at 488 and 546 nm, respectively. DAPI illumination was achieved with two-photon illumination at 750 nm. 12-bit raw confocal images were deconvolved using Huygens Deconvolution software (Scientific Volume Image) and maximum likelihood estimation with a signal-to-noise ratio of 5. Deconvolved images were converted from floating point to 16-bit images in ImageJ without scaling, auto-scaled, and converted to 8-bit RGB images. SUMO1 immunoreactivity was intensely bright in the nucleus compared with the plasma membrane. To allow assessment of colocalization of SUMO staining with Kv2.1 staining in the plasma membrane, images of SUMO1 staining were subjected to nonlinear intensity compression (gamma correction) with a gamma value of 0.35. Images with and without primary antibody were scaled identically. Double-stained samples were analyzed in ImageJ using RGB2B colocalization and default settings to generate black RGB images with saturated pixels at sites of colocalization.

For FRET studies, neurons were imaged with a 60× NA 1.40 oil objective on the identical imaging platform. The Leica Acceptor Photobleaching Wizard was used to obtain prebleach images of Kv2.1 (Alexa Fluor 488) and SUMO2/3 (Alexa Fluor 594), to create a region to bleach on the Kv2.1 image, to bleach the Alexa Fluor 594 fluorescence within the region (200 passes of full laser power), and to obtain post-bleaching images of Alexa Fluor 488 and Alexa Fluor 594 fluorescence. Using ImageJ, raw Alexa Fluor 488 images were de-noised, and FRET efficiency images within the bleaching regions were created, on a pixel-by-pixel basis, by subtracting prebleach from post-bleach and then dividing the difference by the post-bleach intensity. Histograms of the calculated FRET efficiencies within the bleaching area were calculated and plotted.

Molecular biology and production of peptides

Rat Kv2.1 (available from GenBank/EMBL/DDBJ under accession no. NM_013186) was subcloned into pMAX, a vector with a CMV promoter (Rajan et al., 2005). Mutations were introduced with Pfu QuickChange PCR (Agilent Technologies). Human $SUMO1_{101}$ (available from GenBank under accession no. BC005899) was cloned as described previously (Rajan et al., 2005). Yellow fluorescent protein (YFP) and cyan fluorescent protein (CFP) genes (Takara Bio Inc.) were inserted into $SUMO1_{101}$ and Kv2.1 at the N termini as described previously for eGFP, and SENP1 and SENP1-C603S were produced as GST fusions as done previously (Rajan et al., 2005). $SUMO1_{101}$, $SUMO1_{95}$, and $SUMO1_{97}$ were produced in pET28a with six-His tags and a tobacco itch virus (TEV) cleavage domain using BL21 (DE3) *Escherichia coli* isolated by routine procedures. The tag was removed with TEV before dialysis against 140 mM KCl, 0.5 mM $CaCl_2$, and 5 mM HEPES, pH 7.4. Protein concentration was determined by BCA assay (Thermo Fisher Scientific). $SUMO2_{92}$ and $SUMO3_{92}$ were purchased from Boston Biochem; like $SUMO1_{97}$, these are matured forms of the proteins. $SUMO1_{101}$ was heat-denatured at 95°C for 15 min.

Electrophysiology

Experiments were performed at 32°C using a feedback-controlled heated perfusion system (Warner Instruments). Whole cell patch clamp was performed as described previously (Plant et al., 2006) using an Axopatch 200B amplifier and pCLAMP software (Molecular Devices) at filter and sampling frequencies of 5 and 25 kHz, respectively, for voltage clamp experiments and 1 and 10 kHz, respectively, for current clamp recording. Electrodes were coated with Sigmacote (Sigma-Aldrich) before use. Voltage clamp errors were minimized with 80% series resistance compensation. Voltage-dependent currents were studied after a P/5 leak-subtraction protocol. Membrane potential and potassium currents were studied with solution A in the bath (in mM): 1.3 $CaCl_2$, 0.5 $MgCl_2$, 0.4 $MgSO_4$, 3.56 KCl, 0.44 KH_2PO_4, 139.7 NaCl, 0.34 Na_2HPO_4, 5.5 glucose, and 10 HEPES, adjusted to pH 7.4 with NaOH. Electrodes were fabricated from borosilicate glass (Clark Electromedical) and had a resistance of 3–5 MΩ when filled with solution B containing (in mM): 136 KCl, 1 $MgCl_2$, 2 K_2ATP, 5 EGTA, and 10 HEPES, adjusted to pH 7.2 with KOH. To study inactivating (I_{KA}) and delayed rectifier (I_{DR}) voltage-gated potassium currents in hippocampal cells, 50 nM tetrodotoxin (Sigma-Aldrich) was included in the bath to block voltage-gated sodium currents. I_{KA} and I_{DR} were isolated with two voltage protocols. First, both currents were evoked by 500-ms test pulses to between −90 and +90 mV from −80 mV. The inclusion of a 250-ms prepulse to −30 mV before the test pulse inactivated I_{KA} and isolated I_{DR}. I_{KA} was assessed in the same cells by subtracting I_{DR} from the total potassium current. Sodium currents were studied as described previously (Plant et al., 2006), using bath solution C comprising (in mM): 130 NaCl, 5 CsCl, 2 $CaCl_2$, 1.2 $MgCl_2$, 5 glucose, and 10 HEPES, adjusted to pH 7.4 with NaOH. The electrode solution D contained (in mM): 60 CsCl, 80 CsF, 10 EGTA, 1 $CaCl_2$, 1 $MgCl_2$, 5 Na_2ATP, and 10 HEPES, adjusted to pH 7.4 with CsOH. For macropatch recording, 1.5–2-MΩ electrodes were filled with solution A, and the inside of excised patches was perfused with solution B containing the indicated peptides. To calibrate the rate of exchange at the inside face of macropatches on bath perfusion, Kv2.1 was studied with 15 mM TEA and half-block was observed at 1.2 ± 0.8 s for $n = 4$ cells studied.

Live CHO cell FRET and single-particle photobleaching

FRET interaction at the cell surface was assessed with CFP-tagged K2P1 and YFP-SUMO1 using an automated fluorescence microscope (IX81; Olympus). CFP was excited at 458 nm, and the emission was collected through a 470–500-nm bandpass filter. YFP was excited at 514 nm, and the emission was collected through a 525–575-nm bandpass filter. Experiments were controlled with Metamorph (Molecular Devices), and images were captured using an EM-CCD camera and analyzed offline with ImageJ. CFP was photobleached by continuous excitation, and the mean time–constant (τ) was determined from two to five selected regions studied from each cell by images captured every 5 s with a 200-ms exposure. In live cells, FRET is achieved only when proteins interact directly (Sekar and Periasamy, 2003). Here, we measured macroscopic donor decay time course, a FRET strategy

that limits inaccuracies that result from differences in initial acceptor and donor intensities and acceptor bleaching (Jares-Erijman and Jovin, 2003).

Single particles at the cell surface were observed using total internal reflection fluorescent (TIRF) microscopy. Green fluorescent protein (GFP) was excited by a 488-nm, 10-mW argon laser (CVI Melles Griot), and the critical angle for TIRF was adjusted by hand using a micrometer and a high numerical aperture apochromat objective (150×, 1.45 NA; Olympus) on a fluorescence microscope (IX70; Olympus). To observe single particles, GFP-fused subunits were expressed at lower levels than those for electrophysiology and FRET studies. Constant excitation was used to induce photobleaching in a discrete, stepwise manner. Movies of 300–500 frames were acquired at 10 Hz using a back-illuminated EM-CCD camera. Data were analyzed according to Ulbrich and Isacoff (2007). Average background fluorescence was determined from the first five images and subtracted from the movie. Then, fluorescence was summed for a 4 × 4 pixel region around the peak intensity pixel of each particle studied and plotted against time using ImageJ and Origin (version 6) software.

Mass spectrometry (MS)

Similar to the strategy used to study K2P1 (Plant et al., 2010), a modified pET28a vector (Invitrogen) carrying rat Kv2.1 residues 411–853 was coexpressed in *E. coli* with pT-E1E2S1(T95K), a vector carrying mouse SUMO-activating enzyme (SAE)1 and SAE2 (as a linear fusion of Aos1 and Uba2), SUMO-conjugating enzyme (Ubc9), and SUMO1 (Uchimura et al., 2004) that we altered per Knuesel et al. (2005) to $SUMO1_{97}$(T95K). Proteins were purified, digested, and analyzed on an Ultimate 3000 Nano-HPLC (Dionex) and LTQ-FT tandem MS (Thermo Fisher Scientific) running Xcalibur (version 2.2). A detailed description of biochemistry, protein identification, and tandem MS sequencing are in the supplemental text (Fig. S6).

Online supplemental material

Table S1 lists the biophysical parameters for native I_{Na} and I_{KA} currents in hippocampal neurons at baseline and after intracellular application of 75 pM $SUMO1_{101}$ or 250 pM SENP1. Table S2 lists the biophysical parameters for four Kv2.1 channels with point mutations (K145Q, K255Q, K470R, or D472A) studied in CHO cells under control conditions and after intracellular application of wild-type and mutant SUMOs and SENPs. Table S3 lists the biophysical parameters for hippocampal neurons at baseline and after intracellular application of wild-type and mutant SUMOs and SENPs. Table S4 lists the biophysical parameters for neurons transiently expressing Kv2.1 or Kv2.1-K470Q channels at baseline and after intracellular application of various concentrations of active or heat-denatured $SUMO1_{101}$.

Fig. S1 shows the effects of SUMO2 and SUMO3 on the firing rates of hippocampal neurons, the biophysical attributes of native I_{DR}, and the operation of Kv2.1 and Kv2.1-K470Q channels

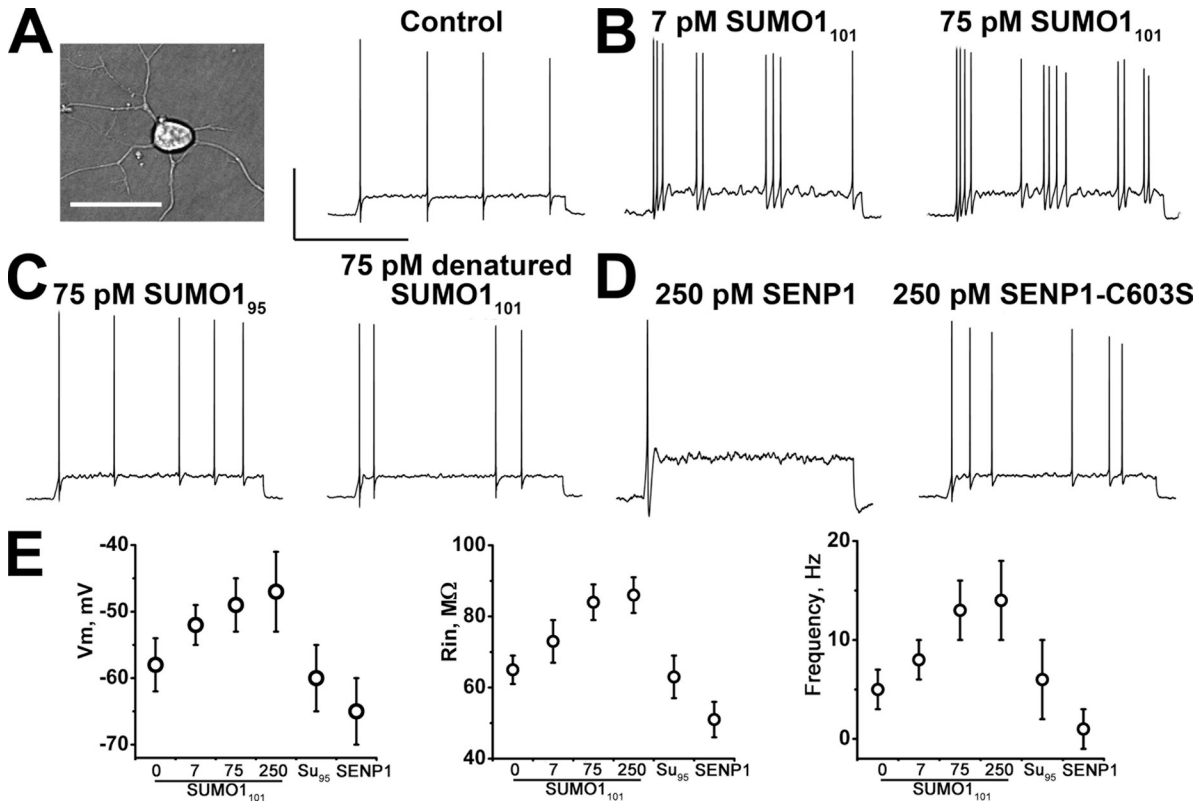

Figure 1. SUMO1 modulates the excitability of hippocampal neurons. Rat hippocampal neurons exposed via the pipette to $SUMO1_{101}$, $SUMO1_{95}$, heat-denatured $SUMO1_{101}$, SENP1, or SENP1-C603S and assessed for Vm, R_{IN}, and Ff (with 2-s current injections of 10 pA) in whole cell mode. Recording conditions (Plant et al., 2006) and biophysical parameters are in Table I. Bars in A are 50 mV and 1 s, and also apply to B–D. (A) Photomicrograph of a neuron (left); bar, 20 µm. Evoked action potentials under baseline conditions (right). (B) Action potential firing increases in frequency with 7 pM $SUMO1_{101}$ in the pipette (left) and is increased further with 75 pM $SUMO1_{101}$ (right). (C) Ff is insensitive to linkage-incompetent $SUMO1_{95}$ (left) and heat-denatured $SUMO1_{101}$ (right). (D) Excitability is dampened by 250 pM SENP1 (left), but not by inactive SENP1-C603S (right). (E) Mean ± SEM Vm (left), R_{IN} (middle), and Ff (right) for 8–20 cells studied with the indicated proteins (Table I).

in CHO cells under control conditions. Fig. S2 shows immunostaining and colocalization of native Kv2.1 and SAE1 or Kv2.1 and Ubc9 in hippocampal neurons. Fig. S3 shows that I-V and G-V relationships for Kv2.1-K145Q and Kv2.1-K255Q channels under control conditions and after intracellular application of 75 pM $SUMO1_{101}$ or 250 pM SENP1 are like those observed for wild-type channels; biophysical parameters are listed in Table S2. Fig. S4 shows that 75 pM $SUMO1_{101}$ and 250 pM SENP1 have no effect on Kv2.1 channels with the mutation K470R or D472A in the Kv2.1 sumoylation site; biophysical parameters are listed in Table S2. Fig. S5 shows that neither 75 pM $SUMO1_{101}$ nor 250 pM SENP1 alters the inactivation of Kv2.1 or Kv2.1-K470Q channels. Fig. S6 demonstrates the conjugation of SUMO1 to K470 in the C-terminal portion of Kv2.1 ($Kv2.1_{410\text{-}853}$) via MS and tandem MS sequence analysis. The online supplemental material is available at http://www.jgp.org/cgi/content/full/jgp.201110604/DC1.

RESULTS

Sumoylation increases excitability of hippocampal neurons

Rat hippocampal neurons in primary culture were studied first using current clamp recording in whole cell mode (Fig. 1 A). This method allowed for the introduction of reagents into the cells via the recording electrode and for the assessment of three measures of excitability: resting membrane potential (Vm), membrane input resistance (R_{IN}), and action potential firing frequency (Ff).

Intracellular application of recombinant $SUMO1_{101}$ increased all three measures of excitability in a concentration-dependent manner (Fig. 1, B and E, and Table I). Under resting conditions, neurons had a mean Vm of −58 mV, a mean R_{IN} of 65 MΩ, and, in response to 2-s current pulses of 10 pA, they fired trains of action potentials with a mean frequency of 5 Hz. Excitability was enhanced partially by 7 pM $SUMO1_{101}$ and fully by 75 and 250 pM $SUMO1_{101}$, the latter producing a mean Vm of −47 mV, a mean R_{IN} of 86 MΩ, and a mean Ff of 14 Hz. Indicating that the effects of $SUMO1_{101}$ were specific, neither $SUMO1_{95}$, a truncated peptide unable to link covalently to target lysine, nor heat-denatured $SUMO1_{101}$, changed excitability (Fig. 1 C).

Because sumoylation increased excitability, we anticipated that lysis of SUMO-target adducts would decrease excitability. Indeed, intracellular application of the desumoylating enzyme SENP1 suppressed the three measures of excitability below resting levels (Fig. 1, D and E, and Table I). With 250 pM SENP1, neurons were hyperpolarized to a mean Vm of −65 mV, had a mean R_{IN} of 51 MΩ, and showed a mean Ff of just 1 Hz. In contrast, application of the inactive enzyme SENP1-C603S, carrying a point mutation in the catalytic site, failed to elicit changes.

SUMO alters the voltage dependence of I_{DR} in hippocampal neurons

Rat hippocampal neurons use a well-defined group of voltage-dependent currents to produce action potentials. The primary currents are the rapidly activating and inactivating voltage-dependent sodium current, I_{Na}, the

TABLE I

Biophysical parameters for hippocampal neurons, native I_{DR} currents, and cloned Kv2.1 channels

Treatment	Hippocampal neurons				Native I_{DR}			Cloned Kv2.1			Cloned K470Q		
	Dose	Vm	Rin	Ff	$V_{1/2}$	V_s	I_{PEAK}	$V_{1/2}$	V_s	I_{PEAK}	$V_{1/2}$	V_s	I_{PEAK}
	pM	*mV*	*MΩ*	*Hz*	*mV*		*pA/pF*	*mV*		*pA/pF*	*mV*		*pA/pF*
None		−58 ± 4	65 ± 4	5 ± 2	22 ± 2	14 ± 3	72 ± 12	21 ± 4	9 ± 1	245 ± 16	3 ± 3	13 ± 3	382 ± 24
$SUMO2_{92}$	75	−50 ± 4[a]	87 ± 5[a]	15 ± 5[a]	40 ± 3[b]	13 ± 2	20 ± 7[b]	36 ± 4[b]	10 ± 2	62 ± 10[b]	4 ± 4	11 ± 6	374 ± 21
$SUMO3_{92}$	75	−48 ± 6[a]	86 ± 5[a]	14 ± 4[a]	39 ± 4[b]	12 ± 4	21 ± 7[b]	36 ± 6[b]	9 ± 3	62 ± 11[b]	4 ± 4	11 ± 7	373 ± 20
$SUMO1_{101}$	7	−52 ± 3	73 ± 6	8 ± 2	28 ± 3[a]	12 ± 3	35 ± 8[b]	28 ± 3[a]	12 ± 3	100 ± 15[b]	4 ± 8	13 ± 4	378 ± 17
$SUMO1_{101}$	75	−49 ± 4[a]	84 ± 5[a]	13 ± 3[a]	39 ± 3[b]	12 ± 3	22 ± 8[b]	37 ± 4[b]	10 ± 2	61 ± 8[b]	4 ± 3	11 ± 4	375 ± 19
$SUMO1_{101}$	250	−47 ± 6[a]	86 ± 5[a]	14 ± 4[a]	37 ± 4[b]	11 ± 4	21 ± 9[b]	35 ± 6[b]	9 ± 4	63 ± 9[b]	3 ± 4	12 ± 6	370 ± 24
$SUMO1_{95}$	75	−60 ± 5	63 ± 6	6 ± 4	20 ± 3	13 ± 3	73 ± 7	20 ± 3	13 ± 3	249 ± 11	5 ± 4	13 ± 3	372 ± 15
denatured $SUMO1_{101}$	75	−57 ± 5	64 ± 3	5 ± 2	19 ± 4	12 ± 3	70 ± 8	20 ± 5	11 ± 4	240 ± 20	4 ± 4	13 ± 3	378 ± 18
SENP1	250	−65 ± 5[a]	51 ± 5[a]	1 ± 2[a]	3 ± 4[b]	13 ± 4	100 ± 18[b]	1 ± 4[b]	10 ± 2	370 ± 23[b]	4 ± 4	13 ± 4	366 ± 21
SENP1-C603S	250	−57 ± 5	64 ± 6	6 ± 3	20 ± 4	13 ± 4	72 ± 14	19 ± 6	9 ± 3	249 ± 17	4 ± 3	13 ± 3	388 ± 21
Δ SENP-SUMO		16 ± 6	33 ± 8	12 ± 4	36 ± 5	0 ± 5	78 ± 20	36 ± 6	0 ± 3	309 ± 24	0 ± 5	0 ± 6	9 ± 28

Neurons (Figs. 1 and 2) and cloned channels in CHO cells (Fig. 4) were studied in whole cell mode using filter and sampling frequencies of 5 and 25 kHz for voltage clamp studies and 1 and 10 kHz for current clamp recording. Voltage-dependent currents were studied after a P/5 leak subtraction. Stimulation protocols are described in the figure legends. Membrane potential and potassium currents were studied in solution A (in mM): 1.3 $CaCl_2$, 0.5 $MgCl_2$, 0.4 $MgSO_4$, 3.56 KCl, 0.44 KH_2PO_4, 139.7 NaCl, 0.34 Na_2HPO_4, 5.5 glucose, and 10 HEPES, pH 7.4 with NaOH. Electrodes were filled with solution B (in mM): 136 KCl, 1 $MgCl_2$, 2 K_2ATP, 5 EGTA, and 10 HEPES, pH 7.2 with KOH. Sodium currents were studied with solution C in the bath (in mM): 130 NaCl, 5 CsCl, 2 $CaCl_2$, 1.2 $MgCl_2$, 5 glucose, and 10 HEPES, pH 7.4 with NaOH. The electrode solution D contained (in mM): 60 CsCl, 80 CsF, 10 EGTA, 1 $CaCl_2$, 1 $MgCl_2$, 5 Na_2ATP, and 10 HEPES, pH 7.4 with CsOH. To determine $V_{1/2}$, voltage evoking half-maximal conductance, and V_s, the slope of the curve, the normalized current was plotted against voltage and fitted to the Boltzmann equation, $G = G_{max}/(1+\exp[-(V-V_{1/2})/V_s])$, where G_{max} is maximum conductance. I_{PEAK} was determined at +50 mV. 8–20 cells were studied in each condition. ΔSENP-SUMO is the mean difference between exposure to SENP1 and 75 pM $SUMO1_{101}$. Vm, resting membrane potential; Rin, input resistance; Ff, firing frequency.

[a]Statistical difference determined by comparison to untreated cells using unpaired *t* tests, $P < 0.01$.

[b]Statistical difference determined by comparison to untreated cells using unpaired *t* tests, $P < 0.001$.

rapidly activating and inactivating voltage-dependent potassium current, I_{KA}, and a delayed rectifier potassium current, I_{DR}. Voltage clamp recording was used to determine whether sumoylation altered excitability via changes in one or more of these currents. Neither the magnitude nor kinetics of I_{Na} or I_{KA} were changed significantly by $SUMO1_{101}$, SENP1, heat-denatured $SUMO1_{101}$, or SENP1-C603S (Fig. 2, A and B, and Table S1). In contrast, I_{DR} was significantly altered.

Isolation of I_{DR} from the other currents was achieved by application of 50 nM tetrodotoxin to block I_{Na} and depolarizing prepulses to −30 mV to inactivate I_{KA} (Fig. 2 C). Mean peak I_{DR} current density at 50 mV was 72 pA/pF. The application of $SUMO1_{101}$ decreased I_{DR} in a concentration-dependent manner that saturated with 75 pM at 22 pA/pF (Fig. 2 C and Table I). In reciprocal fashion, 250 pM SENP1 increased peak I_{DR} above baseline to 100 pA/pF. I_{DR} was unaltered by SENP1-C603S or heat-denatured $SUMO1_{101}$.

A principal basis for lower I_{DR} magnitude was a SUMO-induced shift in the voltage required to activate the current (Fig. 2 C and Table I). Thus, the half-maximal activation voltage ($V_{1/2}$) determined from the normalized G-V relationship changed from 3 mV with the desumoylating enzyme to 39 mV with 75 pM $SUMO1_{101}$ (without a change in slope factor, V_s). In the absence of applied SENP1 or $SUMO1_{101}$, I_{DR} had a $V_{1/2}$ of 20 mV, a value midway between the maximal effects of the desumoylating and sumoylating reagents.

SUMO2 and SUMO3 are 95% identical in amino acid sequence and notable for forming polySUMO chains (Ulrich, 2008). SUMO1 is only 50% identical to SUMO2 and links to targets in monomeric fashion (Tatham et al., 2001). Despite these differences, the effects of

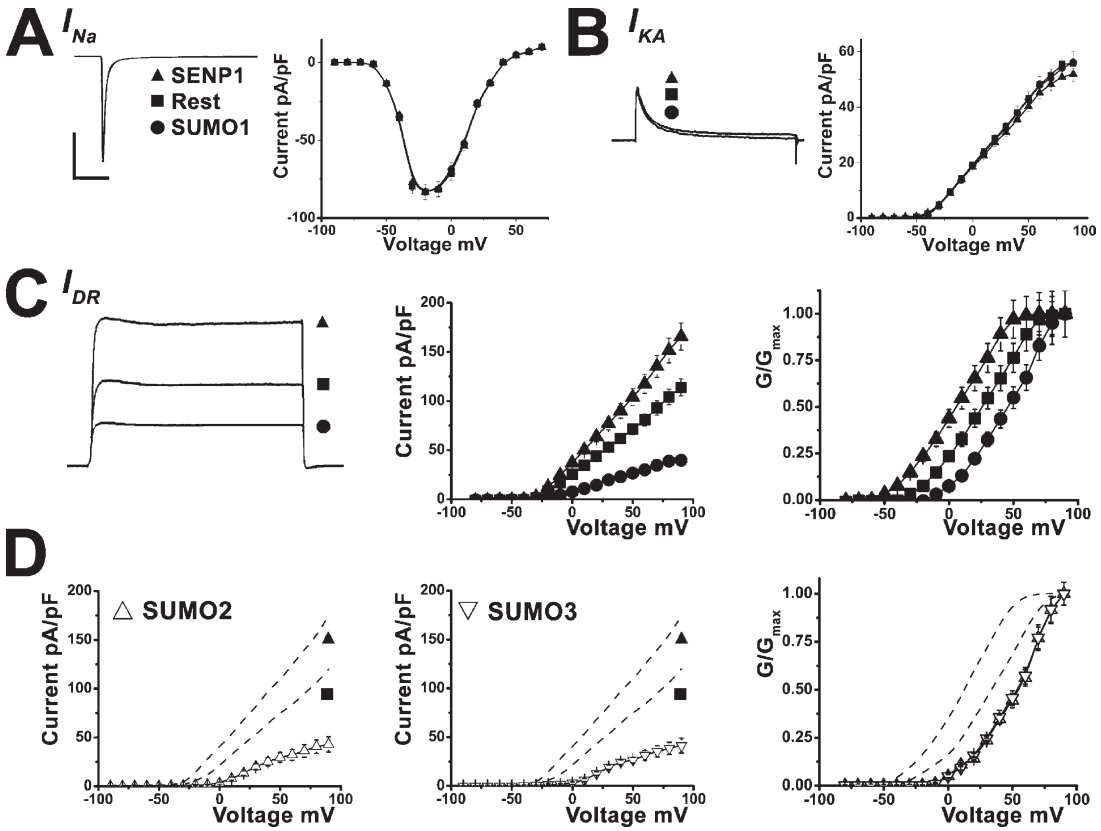

Figure 2. SUMO1 suppresses I_{DR} in hippocampal neurons. Neurons were studied under voltage clamp in whole cell mode, and native I_{Na}, I_{KA}, and I_{DR} were assessed for response to intracellular application of 75 pM $SUMO1_{101}$ (●), with heat-denatured $SUMO1_{101}$ (■, Rest), or 250 pM SENP1 (▲). I_{DR} was also assessed for response to 75 pM $SUMO2_{92}$ (△) or $SUMO3_{92}$ (▽). An ensemble current trace and mean I-V relationships and normalized G-V relationships are shown. Recording conditions and biophysical parameters for I_{DR} are shown in Table I; values for I_{Na} and I_{KA} are in Table S1. Bars represent 1 nA and 10 ms in A and 1 nA and 100 ms in B and C. (A) I_{Na} magnitude and I-V relationships were unaltered by $SUMO1_{101}$ or SENP1. Protocol: 50-ms test pulses to −10 from −80 mV every 10 s (n = 10 –14 cells). (B) I_{KA} magnitude and I-V relationships were unaltered by $SUMO1_{101}$ or SENP1. Protocol: 500-ms test pulses to +50 from −80 mV every 10 s to activate both I_{KA} and I_{DR}, followed by repetition with an additional 250-ms pulse to −30 mV before the test pulse to inactivate I_{KA} and isolate I_{DR}. I_{KA} was determined by subtracting I_{DR} from the total potassium current in the presence of 50 nM tetrodotoxin to remove contaminating sodium currents (n = 10–20 cells). (C) I_{DR} magnitude was augmented by SENP1, unaltered by heat-denatured $SUMO1_{101}$, and diminished by $SUMO1_{101}$. The difference in the midpoint of the G-V relationships with SENP1 (n = 20 cells) and $SUMO_{101}$ (n = 10 cells) was 36 ± 5 mV. (D) I_{DR} magnitude was diminished by SUMO2 and SUMO3. The difference in the midpoint of the G-V relationships between SENP1 (C) and $SUMO2_{92}$ (n = 10 cells) was 37 ± 7 mV, and it was 37 ± 1 mV between SENP1 and $SUMO3_{92}$ (n = 10 cells).

intracellular application of 75 pM SUMO2 and 75 pM SUMO3 on hippocampal Vm, R_{IN}, Ff, and mean peak I_{DR} density were found to be like those observed with 75 pM $SUMO1_{101}$ (Table I, Fig. 2 D, and Fig. S1).

Association of native Kv2.1 with SUMO at the neuronal cell surface

Because Kv2.1 channels pass I_{DR} in rat hippocampal neurons (Murakoshi and Trimmer, 1999), immunostaining and microscopy were used to determine the subcellular localization of native Kv2.1 and SUMOs. As described by Lim et al. (2000), neuronal Kv2.1 was visualized by wide field microscopy at the plasma membrane in soma and proximal dendrites in large clusters and outside of these domains (Fig. 3 A). Thin-slice confocal imaging demonstrated neuronal SUMO2 and/or SUMO3 (the antibody recognizes both isoforms) throughout the cells and colocalized with Kv2.1 at the cell surface (Fig. 3 A, a). SUMO1 immunoreactivity was most intense in the nucleus, observed in the cytosol, and visualized to colocalize with Kv2.1 in scattered foci at the plasma membrane (Fig. 3 A, b). Immunoreactivity to the SUMO pathway enzymes, SAE1 and Ubc9, was observed to be distributed throughout the neurons, with comparatively sparse colocalization at the cell surface with Kv2.1 (Fig. S2).

Conventional confocal microscopy, as performed here at the limits of diffraction, identifies two proteins as colocalized even when they are separated by up to 200 nm; therefore, colocalization indicates proximity and does not require protein–protein contact. In contrast, FRET reports on short distances (1–10 nM) achieved when proteins interact directly. To confirm that endogenous Kv2.1 and SUMO associate in hippocampal neurons, we used antibody-mediated FRET (Kenworthy, 2001). Antibodies linked to Alexa Fluor 488 (for Kv2.1) and Alexa Fluor 594 (for SUMO2/3) were used as donor and acceptor, respectively. Photobleaching of the acceptor (leading to increased donor fluorescence) revealed close interaction of native Kv2.1 and SUMO2/3 (Fig. 3 B) in three subcellular locales: within Kv2.1 clusters (open arrow), at the periphery of Kv2.1 clusters (solid arrow), and at the surface distant from clusters (arrowhead). Specificity of the measurements was demonstrated by the failure to observe FRET when neurons were stained for Kv2.1 and the highly expressed cytosolic enzyme GAPDH (Fig. 3 C). Because FRET efficiency using this method depends not only on distance but also on the degree of saturation of antigen with antibody, the distance between Kv2.1 and SUMO2/3 antibodies could be judged to be <10 nm, consistent with direct protein–protein association, but not more accurately (Kenworthy, 2001).

SUMO alters the operation of cloned Kv2.1 in CHO cells as it does neuronal I_{DR}

To determine if Kv2.1 channels responded to SUMOs in the same fashion as neuronal I_{DR}, cloned rat Kv2.1 was transiently expressed in CHO cells. Kv2.1 currents were diminished by intracellular $SUMO1_{101}$ in a concentration-dependent manner and were enhanced by SENP1 (Fig. 4 A and Table I). Baseline currents rested between levels observed with $SUMO1_{101}$ and SENP1. Thus, Kv2.1 channels in CHO cells had a mean peak current at 50 mV of 245 pA/pF before treatment; mean peak currents decreased to 61 pA/pF with 75 pM $SUMO1_{101}$ and increased to 370 pA/pF with 250 pM SENP1. Kv2.1 channel G-V relationships also changed like neuronal I_{DR} (Fig. 4 A and Table I). Thus, $V_{1/2}$ for Kv2.1 in CHO cells treated with SENP1 was 1 mV; this shifted maximally with 75 pM $SUMO1_{101}$ to 37 mV, and channels in untreated cells were poised between these values at 21 mV. Also like neuronal I_{DR}, exposure to 75 pM SUMO2 or 75 pM SUMO3 had the same effects on cloned Kv2.1 channels as 75 pM $SUMO1_{101}$. SENP1-C603S and heat-denatured $SUMO1_{101}$ did not alter current–density or G-V relationships for Kv2.1 channels (Table I). Further, CHO cells without overexpressed Kv2.1 channels showed no changes with either 75 pM $SUMO1_{101}$ or 250 pM SENP1 (not depicted).

SUMO1 regulates Kv2.1 via K470

To locate the lysine(s) that mediates SUMO regulation of Kv2.1, the primary sequence was examined and three high probability sites for modification were identified: K145, K255, and K470. Each site was mutated separately to glutamine (Q), and the altered channels were studied in CHO cells. Mutating K145 or K255 had no significant effect yielding channels that behaved like wild type in terms of current magnitude, voltage dependence, and sensitivity to SUMO pathway regulation (Fig. S3 and Table S2). Thus, K145Q and K255Q channel currents were diminished ~75% by 75 pM $SUMO1_{101}$, augmented ~50% by 250 pM SENP1, and showed ~36-mV shifts in $V_{1/2}$ between the two conditions.

In marked contrast, Kv2.1-K470Q channels were insensitive to regulation by sumoylation (Fig. 4 A and Table I). Moreover, the $V_{1/2}$ for K470Q channels was 4 mV, similar to desumoylated wild-type channels, and this parameter was unaltered by exposure to 75 pM $SUMO1_{101}$, SUMO2, or SUMO3, or 250 pM SENP1. Given the similar impact of the three SUMO isoforms on Kv2.1 in CHO cells, and the array of SUMO1 reagents validated by prior use (Plant et al., 2010), SUMO1 was employed hereafter.

Two other mutations used to suppress sumoylation of classical nuclear substrates were studied. First, K470 in Kv2.1 was retained, but the canonical negative residue in the +2 position of the sumoylation motif ($AK^{470}KD$) was neutralized (D472A) (Rodriguez et al., 2001; Sapetschnig et al., 2002); second, K470 was altered to arginine (K470R), maintaining the basic character of the side chain but eliminating the ε-amino group that is sumoylated. Consistent with suppression of sumoylation

of K470, both D472A and K470R channels behaved like K470Q channels and were insensitive to 75 pM $SUMO1_{101}$ and 250 pM SENP1 (Fig. S4 and Table S2). With long test pulses, wild-type Kv2.1 channels inactivated slowly, showing a mean time constant (τ) for inactivation of 9.9 ± 1.8 s; this was unaltered by 75 pM $SUMO1_{101}$ or 250 pM SENP1 (Fig. S5). Similarly, K470Q channels inactivated with a τ of 10 ± 1.5 s and were unaffected by $SUMO1_{101}$ or SENP1.

To confirm that Kv2.1-K470 was necessary and sufficient to control excitability via SUMO in the native milieu, cloned channels were transiently overexpressed in hippocampal neurons (Fig. 4 B and Table S3). Neurons expressing these clones were hyperpolarized compared with untreated cells. Therefore, to blunt potassium flux and facilitate action potential firing, tetraethylammonium was added to the bath. With 7 pM of intracellular $SUMO1_{101}$, neurons with cloned wild-type Kv2.1 channels showed a depolarizing rise in Vm and an increase in R_{IN}, and they began to fire action potentials. All three effects were augmented with 75 pM $SUMO1_{101}$. In contrast, cells heterologously expressing Kv2.1-K470Q channels showed no changes in Vm, R_{IN}, or Ff with either concentration of $SUMO1_{101}$.

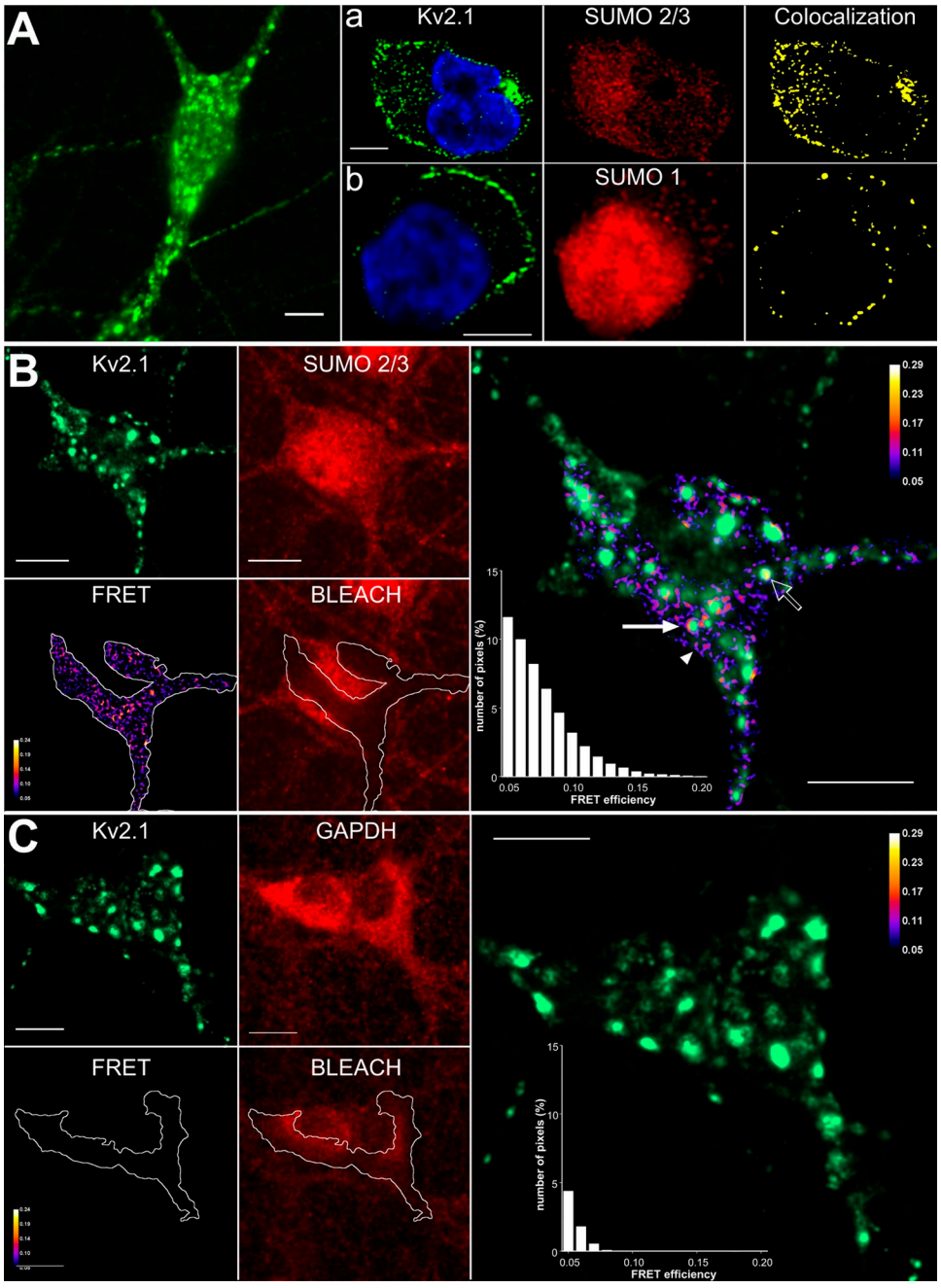

Figure 3. FRET between native Kv2.1 and SUMO2/3 in hippocampal neurons. Cultured rat hippocampal neurons were studied by immunostaining and confocal microscopy or acceptor photobleaching, antibody-mediated FRET. Bars in all panels are 10 µm. (A) Wide field photomicrograph showing Kv2.1 in clusters and outside the domains. (a) Dense colocalization of Kv2.1 and SUMO2/3 by thin-section microscopy (0.48-µm slices). (Left) Kv2.1 (green) and nuclear (blue) stain. (Middle) SUMO2/3. Right: Colocalization of Kv2.1 and SUMO2/3. (b) Kv2.1 and SUMO1 imaged, processed, and colocalized as in panel a. (B) Acceptor photobleaching showing FRET between Kv2.1 and SUMO2/3 in 2.48-µm sections. (Left panels) *Kv2.1* visualized with Alexa Fluor 488 (green); *SUMO2/3* visualized with Alexa Fluor 594 (red); and *BLEACH* shows the region where Alexa Fluor 594 was photobleached (white line). *FRET* efficiency calculated for pixels within the bleached area. (Right) Overlay of Kv2.1 and FRET reveals Kv2.1 with SUMO2/3 within (open arrow), at the periphery (solid arrow), and at the cell surface distant from Kv2.1 clusters (arrowhead). Inset is a histogram of the distribution of FRET efficiency for pixels in the bleached region. Pixels with an efficiency <5% are not shown. (C) Acceptor photobleaching demonstrating the absence of FRET between Kv2.1 and GAPDH, a cytosolic protein. Images were obtained, analyzed, and presented as in B.

Regulation of Kv2.1 is repetitively reversible

To form an isopeptide bond, $SUMO1_{101}$ is matured by C-terminal proteolysis to 97 residues ($SUMO1_{97}$), activated by the SAE1–SAE2 complex, and linked via a thioester bond to C93 of the conjugating enzyme Ubc9. Ubc9 catalyzes formation of a covalent bond between the terminal glycine of $SUMO1_{97}$ and the ε-amino group of lysine on the target. Reversible activation and suppression resulting from desumoylation and resumoylation were shown previously for human K2P1 channels in patches excised from CHO cells (Plant et al., 2010). Here, SUMO regulation of surface Kv2.1 channels was also found to be reversible and independent of the cell cytoplasm and nucleus (Fig. 4 C). Kv2.1 channels expressed in CHO cells and studied in inside-out off-cell patches showed increased current from a mean resting level of 104 ± 11 to 150 ± 19 pA upon the application of 250 pM SENP1 ($n = 6$ patches). Subsequent exposure to 75 pM $SUMO1_{101}$ decreased current to 74 ± 9 pA. The reapplication of SENP1 restored current to 147 ± 14 pA. The same stepwise protocol produced no changes in patches with Kv2.1-K470Q channels (111 ± 9 pA; $n = 4$ patches).

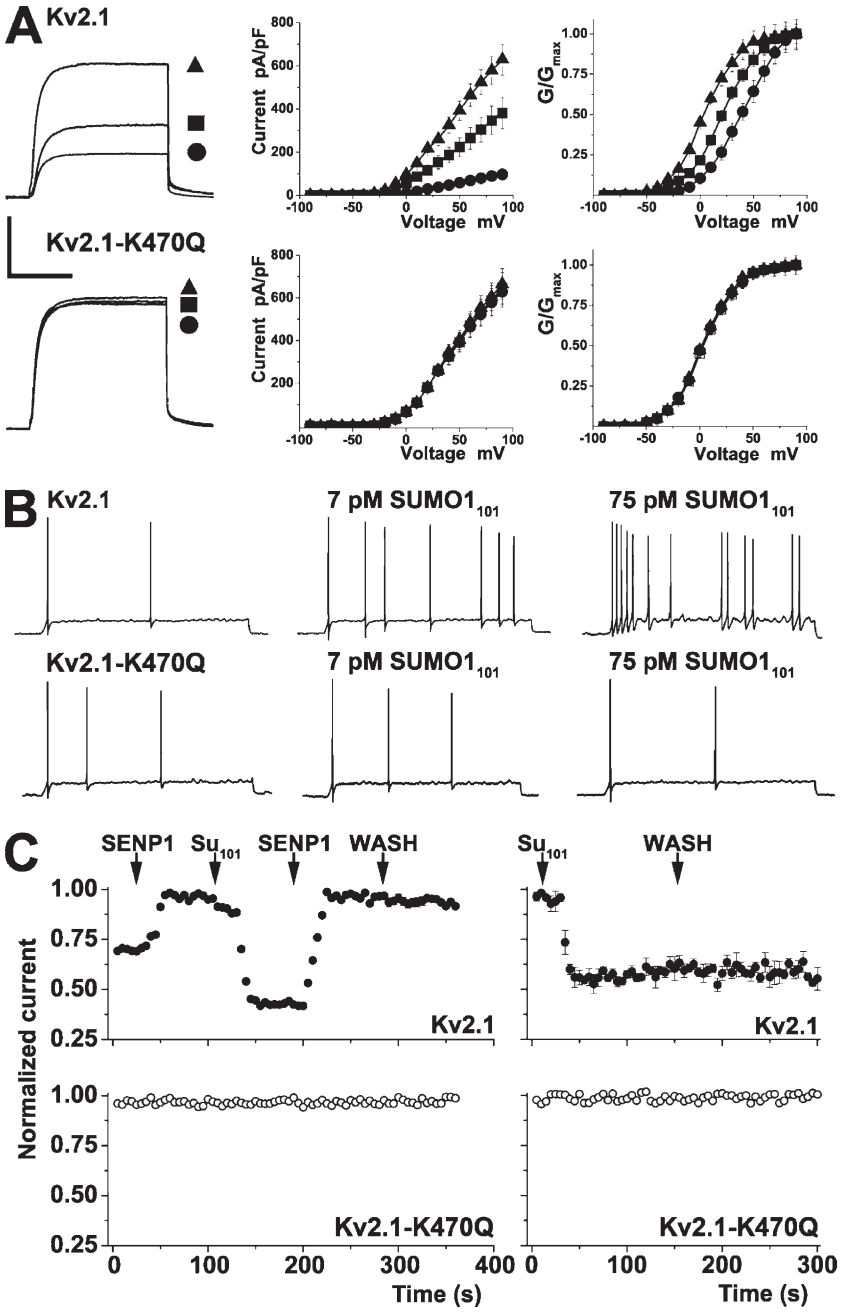

Figure 4. SUMO1 regulates the voltage dependence of Kv2.1 via K470. Whole cell recording with solution A in the bath and solution B in the pipette (Table I); macropatch electrodes were filled with solution A, and the perfusate was solution B with peptides. (A) Kv2.1 or Kv2.1-K470Q channels studied in CHO cells in whole cell mode under control conditions (■; $n = 15$ cells), with 75 pM $SUMO1_{101}$ (●; $n = 12$), or with 250 pM SENP1 in the pipette (▲; $n = 12$) with 500-ms test pulses to 50 from −80 mV every 10 s. (Left) Current traces. (Middle) Mean I-V relationships. (Right) Normalized G-V relationships. Biophysical parameters are summarized in Table I. Bars are 2 nA and 200 ms. Standard error bars are within symbols where not visible. Wild-type Kv2.1 channels showed a 36 ± 6–mV shift between exposure to $SUMO1_{101}$ and SENP1, whereas K470Q channels were insensitive to both reagents. (B) Kv2.1 or Kv2.1-K470Q channels expressed in hippocampal neurons and studied as in Fig. 1, with 5 mM TEA in the bath. (Top) Neurons with Kv2.1 channels show increased activity with 7 pM $SUMO1_{101}$ and 75 pM $SUMO1_{101}$. (Bottom) Neurons with Kv2.1-K470Q channels were insensitive to 7 pM $SUMO1_{101}$ and 75 pM $SUMO1_{101}$. Values for Vm, R_{IN}, and Ff are in Table S3. (C) Kv2.1 or Kv2.1-K470Q channels studied in CHO cells in excised plasma membrane patches. (Top left) Wild-type Kv2.1 channel currents ($n = 6$) increased from a mean starting value of 104 ± 11 to 150 ± 19 pA upon the application of 250 pM SENP1 (first arrow), with a half-maximal effect in 6 ± 2 s. Subsequent application of 75 pM $SUMO1_{101}$ (second arrow) suppressed current to 74 ± 9 pA, with a half-maximal effect in 8 ± 3 s. The reapplication of SENP1 (third arrow) restored current to 147 ± 14 pA, a level that was stable despite washout of SENP1 (WASH). Half-block of Kv2.1 in excised patches by 15 mM TEA in the bath was 1.2 ± 0.8 s ($n = 4$ cells). (Bottom left) Kv2.1-K470Q channels ($n = 4$) had a mean starting value of 111 ± 9 pA and were not altered during the five-phase regimen in the top panel. (Top right) Wild-type Kv2.1 channel currents ($n = 4$) are suppressed (mean starting value, 140 ± 21 pA/pF; $n = 4$ patches) by 75 pM $SUMO1_{101}$, and the effect is stable on the washout of SUMO1 peptide (WASH). (Bottom right) $SUMO1_{101}$ had no effect on Kv2.1-K470Q channel currents (mean starting value, 124 ± 13 pA/pF; $n = 4$).

MS demonstrates sumoylation of Kv2.1 K470

Because K470 is in a non-canonical sumoylation site ($AK^{470}KD$; the −1 site is usually a large hydrophobic residue rather than alanine), we employed MS to confirm conjugation of SUMO to K470 within the motif. As for K2P1 (Plant et al., 2010), we used a bacterial system developed by others to produce SUMO-target conjugates for crystallization (Uchimura et al., 2004). We modified their tri-cistronic plasmid expressing the SAE complex and Ubc9 to carry $SUMO1_{97}T95K$, a mutant that leaves a diglycine remnant of SUMO on the ε-amino group of target lysine after trypsin treatment (Knuesel et al., 2005). $SUMO1_{97}T95K$ was confirmed to regulate Kv2.1 channels like wild-type $SUMO1_{101}$ (not depicted). The intracellular C-terminal portion of Kv2.1 that carries K470 ($Kv2.1_{410\text{-}853}$) was coexpressed from a second plasmid. Affinity purification, SDS-PAGE, and Coomassie blue staining showed a band at the expected apparent mass, ∼65 kD; excision, trypsin treatment, and MS confirmed the band to be $Kv2.1_{410\text{-}853}$–$SUMO_{97}T95K$, with sequence coverage of 60% for Kv2.1 and 28% for SUMO1 (Fig. S6). The spectrum included a mass/charge (m/z) peak at 482.25^{+2} Da, the predicted mass of the fragment bearing K470 linked via its side-chain to the G–G remnant of $SUMO1_{97}T95K$. Sequencing by MS/MS identified the three-ended product uniquely.

FRET between Kv2.1 and SUMO1 at the surface of live cells requires K470

Seeking to confirm intimate association of $SUMO1_{101}$ and Kv2.1 in the plasma membrane of live CHO cells, FRET was used as before with K2P1 (Plant et al., 2010). When tagged with CFP and YFP, CFP-Kv2.1 and CFP-Kv2.1-K470Q subunits were readily observed at the CHO cell surface (Fig. 5 A), a location where native SAE1–SAE2, Ubc9, and SUMO1 have been demonstrated previously (Plant et al., 2010). Consistent with sumoylation of CFP-Kv2.1 by YFP-$SUMO1_{101}$, their coexpression produced donor photobleaching time constants >20 s. In contrast, coexpression of CFP-Kv2.1 with linkage-incompetent YFP-$SUMO1_{95}$ or free YFP yielded similar decay time constants <10 s (Fig. 5, A and B). Reflecting assembly of heteromeric channels in the plasma membrane, coexpression of CFP-Kv2.1-K470Q with YFP-Kv2.1-K470Q subunits demonstrated time constants >20 s. Conversely, coexpression of CFP-Kv2.1-K470Q with YFP-$SUMO1_{101}$ failed to prolong donor decay. This finding supports two conclusions: FRET between Kv2.1 and $SUMO1_{101}$ requires K470, and no other lysine in Kv2.1 is subject to sumoylation.

Ubc9 conjugase fails to bind to the classical SUMO substrate RanGAP1 (Sampson et al., 2001) and will not bind to K2P1 (Plant et al., 2010) when the target lysine in either protein is mutated. In similar fashion, coexpression of YFP-Ubc9 and CFP-Kv2.1 channels yielded elevated photobleaching time constants consistent with the binding of the enzyme to the channel, whereas CFP-Kv2.1-K470Q subunits coexpressed with YFP-Ubc9 showed no evidence for stable interaction (Fig. 5 B).

Two SUMO1 monomers per Kv2.1 channel yield a maximal response

Combining TIRF microscopy and stepwise photobleaching of GFP-tagged subunits allows for visualization of single-ion channels at the cell surface and counting of the assembled subunits. We have previously used this

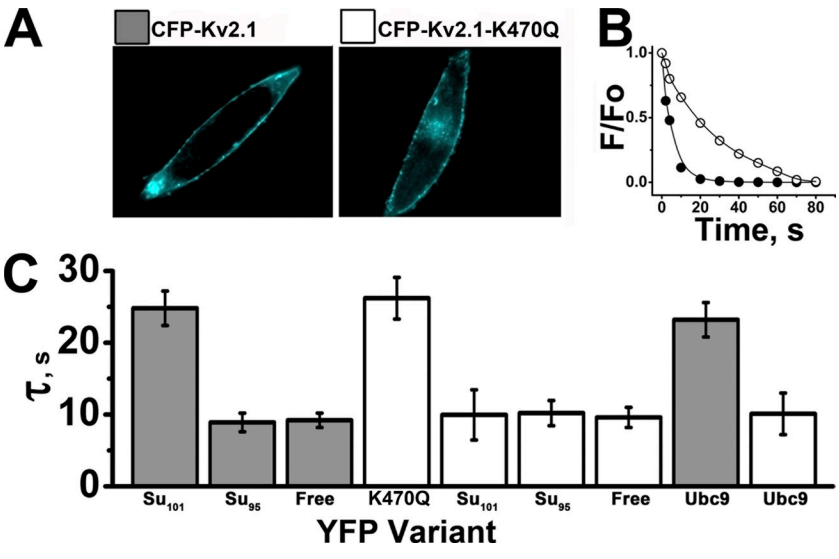

Figure 5. K470 is required for the interaction of Kv2.1 with SUMO or Ubc9. CFP-Kv2.1 and CFP-Kv2.1-K470Q channels were studied with YFP fused to Kv2.1-K470Q, $SUMO1_{101}$, or Ubc9. Data are the mean time constant for CFP decay ± SEM for two to five areas of five to seven cells with continuous excitation. (A) CHO cells expressing CFP-Kv2.1 or CFP-Kv2.1-K470Q. Bar, 10 µm. (B) Exponential decay curves for CFP-Kv2.1 coexpressed with YFP-$SUMO1_{101}$ (○) or free YFP (●). The decrease in normalized fluorescence intensity was fit by a single exponential to give the decay time constant (τ). (C) FRET was observed (mean τ ± SEM) between CFP-Kv2.1 (dark gray) and YFP-$SUMO1_{101}$ (Su_{101}) when K470 was present and SUMO1 was competent to form isopeptide bonds. The mean τ for CFP-Kv2.1 decay was increased upon expression with YFP-$SUMO1_{101}$ (24.8 ± 2.4 s), but not upon expression with YFP-$SUMO1_{95}$ (Su_{95}, τ = 8.9 ± 1.3 s) compared with free YFP (Free; τ = 9 ± 1.1 s). Increased mean τ ± SEM upon expression of CFP-Kv2.1-K470Q (white) and YFP-Kv2.1-K470Q reflects channels with both subunits (τ = 26.2 ± 2.9 s). Unlike CFP-Kv2.1, the mean τ of CFP-Kv2.1-K470Q was not significantly altered by coexpression with YFP-$SUMO1_{101}$ (τ = 10 ± 3.5 s), YFP-$SUMO1_{95}$ (τ = 10.2 ± 1.8 s), or free YFP (τ = 9.2 ± 1.0 s). The interaction of CFP-Kv2.1 with YFP-Ubc9 requires K470; thus, the mean τ was greater for CFP-Kv2.1 (dark gray; τ = 23.2 ± 2.4 s) than for CFP-Kv2.1-K470Q (white; τ = 10 ± 2.9 s).

technique to confirm the dimeric stoichiometry of K2P1 channels and to demonstrate that single, fully sumoylated K2P1 channels at the plasma membrane of CHO cells carry two SUMO1 monomers (Plant et al., 2010). Here, we apply the strategy to SUMO1 and Kv2.1 channels. First, single particles in cells expressing wild-type GFP-Kv2.1 subunits or GFP-Kv2.1-K470Q subunits were confirmed to represent intact channels with four subunits: in both cases, ∼40% of single-channel particles showed four stepwise decreases in fluorescence, whereas three, two, and one step were seen in ∼40, ∼15, and ∼5%, respectively (Fig. 6 A); these were the expected values for a tetrameric Kv channel based on prebleaching, simultaneous bleaching of fluorophores, missed events, and a binomial distribution using GFP at this time resolution (Ulbrich and Isacoff, 2007).

To count SUMO1 monomers on single Kv2.1 channels, untagged Kv2.1 and GFP-tagged $SUMO1_{101}$ were coexpressed (Fig. 6 B); in this case, two bleaching steps were observed for 75% of particles and one bleaching step was observed for 15%, indicative of no more than two GFP-$SUMO1_{101}$ proteins per channel. Providing additional evidence that K470 is required for sumoylation, and that it is the only lysine in Kv2.1 that is modified, Kv2.1-K470Q channels expressed with GFP-$SUMO1_{101}$ yielded no fluorescent particles.

Because photobleaching showed at most two SUMO1 monomers bound to each Kv2.1 channel, despite the presence of four K470 sites (one on each subunit), we sought to verify that Kv2.1 channels modified by just two SUMO1 monomers showed maximal changes in voltage dependence. To do this, Kv2.1 channels were engineered with fewer K470 sites. First, channels with two K470 sites were produced by linking two subunits in series, one with K470 and one with K470Q (Fig. 6 C; Lys-Gln). Channels formed by two Lys-Gln subunits operated like wild-type Kv2.1 channels, showing shifts in $V_{1/2}$ from 3 mV with 250 pM SENP1 to 36 mV with 75 pM $SUMO1_{101}$. Further, ∼75% of these channels showed two bleaching steps when coexpressed with GFP-$SUMO1_{101}$ and ∼15% showed one step, indicating that like wild-type channels with four subunits and four K470 sites, they carried only two SUMO1 molecules. The same SUMO1 stoichiometry and changes in $V_{1/2}$ in response to SENP1 and $SUMO1_{101}$ were observed with dimeric channels formed by subunits linked in the opposite order (Gln-Lys). So, too, a tetrameric construct of four subunits in series with two K470 sites in alternating domains (Lys-Gln-Lys-Gln) bound two GFP-$SUMO1_{101}$ monomers and responded to SENP1 and $SUMO1_{101}$ like wild-type Kv2.1 channels with four sites.

One SUMO monomer gives a partial response

In contrast, one bleaching step was seen when channels were formed by tetrameric constructs with two adjacent SUMO sites (Gln-Lys-Lys-Gln) (Fig. 6 D). In these channels, $V_{1/2}$ shifted from 1 mV with SENP1 to only 13 mV with 75 pM $SUMO1_{101}$. This suggested that the conjugation of two SUMO1 monomers to one channel requires that the two K470 sites be separated by a subunit that was not modified by SUMO1. To confirm that mono-sumoylation and the partial response did not reflect anomalous behavior of this particular channel, other tetrameric constructs with just one K470 site were studied (Lys-Gln-Gln-Gln and Gln-Lys-Gln-Gln). These channels both bound a single GFP-$SUMO1_{101}$ and showed changes in $V_{1/2}$ from 1 mV with 250 pM SENP1 to 16 and 15 mV, respectively, with 75 pM $SUMO1_{101}$. Thus, Kv2.1 channels modified by one rather than two SUMO1 proteins showed a partial shift in activation voltage.

DISCUSSION

Kv2.1 channels, the mediators of I_{DR} current rat hippocampal neurons, are expressed at high levels in virtually all mammalian central neurons and play a prominent role in determining intrinsic excitability through activity-dependent modulation (Misonou et al., 2005). Here, sumoylation of Kv2.1 channels at the neuronal cell surface is shown to suppress excitability as a result of a shift in the $V_{1/2}$ for activation to more depolarized potentials. Desumoylation reverses this effect. Regulation of excitability by modulation of the voltage dependence of Kv channels is a previously recognized response to phosphorylation, second messengers, accessory subunits, drugs, and toxins (Levitan, 1994, 2006; Li-Smerin and Swartz, 1998; Abbott et al., 2001). Because the kinetics of activation and inactivation of Kv2.1 channels are slow compared with I_{Na} and I_{KA}, they are expected to influence firing rates rather than action potential duration. Indeed, sumoylation is found to modify hippocampal neuron Vm, R_{IN}, and Ff, but not action potential duration (Table S3).

A leftward shift in the G-V relationship on desumoylation by SENP1 can fully account for augmentation of peak current magnitudes for neuronal I_{DR} and cloned Kv2.1 channels based on comparison with ionic I-V curves. In contrast, the degree of current suppression by $SUMO1_{101}$ exceeds predictions based on G-V relationships by ∼30–40%. Thus, sumoylation appears to have additional effects on Kv2.1 that diminish current density; possibilities include induction of deep closed states reminiscent of SUMO-mediated silencing of K2P1 channels (Rajan et al., 2005; Plant et al., 2010) that might explain the large fraction of surface Kv2.1 channels in transfected HEK293 cells that show gating currents but do not conduct ions (O'Connell et al., 2010), and reversible effects on channel trafficking, perhaps via an impact of sumoylation on endocytosis (Martin et al., 2007; Kruse et al., 2009).

Although many targets carry SUMO on all available sites before challenge (Hay, 2005), including K2P1 channels (Rajan et al., 2005; Plant et al., 2010), Kv2.1

channels that are less than fully sumoylated are present in cultured neurons and CHO cells. Thus, the $V_{1/2}$ for neuronal I_{DR} and Kv2.1 channels in CHO cells rests midway between the values with SUMO1 or SENP1 and changes rapidly on exposure to the reagents. The notion that the pathway is poised to respond is consistent with swift removal of SUMO from targets by a viral product that inactivates SAE complexes (Boggio et al., 2004). Similarly, heat shock, osmotic challenge, and oxidative stress produce rapid changes in the relative abundance of SUMOs in the cytoplasm and linked to various protein targets (by as-yet undetermined mechanisms) (Bossis and Melchior, 2006; Gareau and Lima, 2010).

Although our studies of Kv2.1 in off-cell patches argue against a required role for other signaling pathways in SUMO regulation, sumoylation and phosphorylation may prove to have an intimate relationship. Supporting the idea, sumoylation of the transcription factor MEF2A (leading to differentiation of postsynaptic dendrites and synapse formation) is phosphorylation dependent in cerebellar granule neurons (Shalizi et al., 2006), and activity-dependent dephosphorylation of MEF2A and MEF2D in hippocampal neurons is associated with excitatory synapse disassembly (Flavell et al., 2006). Suggesting that interaction of the two pathways would be nuanced, phosphorylation takes place at 16 sites in Kv2.1 that have differential effects on gating (Park et al., 2006) and clustering (Misonou et al., 2004, 2005). Of note, sumoylation of some targets is inhibited by lysine acetylation (Shalizi et al., 2006) or ubiquitinylation (Ulrich, 2005).

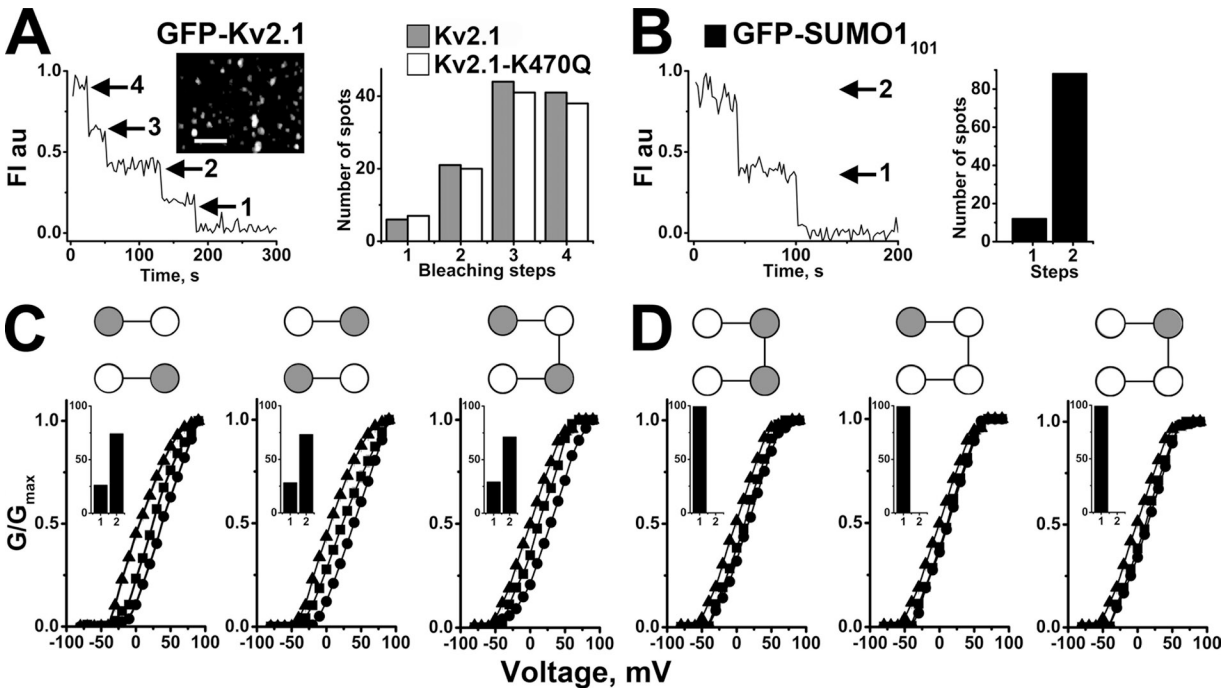

Figure 6. Two SUMO1 monomers associate with Kv2.1 channels to yield a maximal effect. GFP-tagged subunits were studied at the CHO cell surface by TIRF and single-particle photobleaching. Kv2.1 and Kv2.1-K470Q were expressed as monomer, dimer, or tetrameric constructs. G-V relationships for the channels were determined in whole cell mode with control buffer, 250 pM SENP1, or 75 pM $SUMO1_{101}$ in the pipette, as in Fig. 4. (A; left). Time course of photobleaching for a representative GFP-Kv2.1 fluorescent particle showing four steps as expected for a tetrameric channel. (Inset) Fluorescent particles in a cell expressing GFP-Kv2.1. Bar, 60 pixels. (Right) Histogram showing 117 GFP-Kv2.1 particles (gray bars), of which 9% had four bleaching stops, 42% had three, 14% had two, and 5% had a single step. The distribution was similar for 123 GFP-Kv2.1-K470Q particles (white bars), with four, three, two, and one steps at 38, 41, 15, and 6%, respectively. (B; left) Photobleaching time course for a representative GFP-$SUMO1_{101}$ fluorescent Kv2.1 particle showing two bleaching steps with continuous excitation. (Right) Histogram for GFP-$SUMO1_{101}$ expressed with untagged Kv2.1 channels showing that 75% of 80 fluorescent particles had two bleaching steps. No particles with three or more bleaching steps were observed. No discrete immobile particles were observed when GFP-$SUMO1_{101}$ was coexpressed with Kv2.1-K470Q channels. (C) Lys-Gln (gray-white) or Gln-Lys (white-gray) tandem constructs and Lys-Gln-Lys-Gln or Gln-Lys-Lys-Gln tetramer constructs were expressed with GFP-$SUMO1_{101}$. These channels with only two K470 sites showed no more than two bleaching steps. Two steps were recorded in 72% of 50 spots with Lys-Gln channels and 73% of 58 spots with Gln-Lys channels; similar to channels of wild-type monomers, Lys-Gln or Gln-Lys channels showed shifts in $V_{1/2}$ of 34 ± 4 and 35 ± 3 mV (with no change in V_s) between SENP1 and $SUMO1_{101}$ treatment. Similarly, two steps were recorded in 71% of 49 spots for Lys-Gln-Lys-Gln channels and a 33 ± 4–mV shift in $V_{1/2}$ with no change in V_s was observed between SENP1 and $SUMO1_{101}$ exposure. (D) All 49 spots studied with Gln-Lys-Lys-Gln channels and GFP-$SUMO1_{101}$ bleached in a single step. Here, the shift in $V_{1/2}$ between SENP1 and $SUMO1_{101}$ treatment was only 13 ± 8 mV, with no change in V_s. One bleaching step was also observed in all 69 Lys-Gln-Gln-Gln channels and all 58 Gln-Lys-Gln-Gln channels. The total shift in $V_{1/2}$ between SENP1 and $SUMO1_{101}$ treatment for these channels was 15 ± 3 and 14 ± 3 mV, respectively.

A report that Kv2.1 channels in pancreatic β cells and HEK293 cells are suppressed by SUMOs as a result of enhanced inactivation describes widening of action potentials and decreased firing frequency, and does not evaluate voltage-dependent activation (Dai et al. (2009)). In marked contrast, neither our initial description of Kv2.1 sumoylation (Plant et al., 2007) nor this study has revealed changes in the kinetics or magnitude of inactivation (Fig. S4) or action potential duration (Table S3) using concentrations of $SUMO1_{101}$ and SENP1 that produce maximal effects on $V_{1/2}$ of I_{DR} in hippocampal neurons or cloned Kv2.1 channels in CHO cells. A notable difference is that we assessed responses to acute application of recombinant SUMO or SENP1 while they overexpressed YFP-tagged SUMO1 in test cells from a plasmid for days before study; the latter strategy allows for long-term effects of SUMO throughout the cell that may have modified Kv2.1 function in a manner unrelated to direct sumoylation of the channel.

The SUMO pathway at the neuronal cell surface

The observation of SUMO1, SUMO2/3, SAE1, and Ubc9 at the surface of hippocampal neurons with Kv2.1 accords with our observations in *Xenopus laevis* oocytes and CHO cells with K2P1 (Rajan et al., 2005; Plant et al., 2010), and with work by others showing Ubc9 in the dendrites of cultured hippocampal neurons (Martin et al., 2007). As with K2P1, Kv2.1 is regulated by $SUMO1_{101}$ applied to the cytoplasmic surface of off-cell membrane patches. This indicates that the patches carry enzymes that mature $SUMO1_{101}$ to $SUMO1_{97}$, SAE1–SAE2 to activate $SUMO1_{97}$, and Ubc9 to conjugate $SUMO1_{97}$ to the channels; desumoylation required the application of exogenous SENP1. Although known desumoylases affect both SUMO maturation and removal of SUMO from targets (Shen et al., 2006), Kv2.1 in patches remained sumoylated until soluble SENP1 was applied; this suggests that separate enzymes mediate SUMO maturation and desumoylation at the cell surface. The need to apply SENP1 is evocative of ion channels that are intimately associated with protein kinases, but not phosphatases (Levitan, 2006). It is apparent that sumoylation and desumoylation alter the voltage-dependent activation of Kv2.1 channels operating at the plasma membrane and exposed to the external milieu. In contrast, we do not know that all channels visualized at the cell surface by immunostaining and FRET are in the plasma membrane rather than nearby; arguing that the majority are incorporated, our images are similar to those obtained by others studying Kv2.1 in rat hippocampal neurons using antibodies directed toward external channel epitopes (Lim et al., 2000).

Effects of SUMO on other membrane proteins

K2P1 channels are broadly expressed in the central nervous system (Talley et al., 2001), and their silencing by sumoylation (Rajan et al., 2005) was questioned (Feliciangeli et al., 2007) but has been confirmed (Plant et al., 2010). Desumoylation reveals K2P1 to be a canonical potassium-selective leak channel (Ketchum et al., 1995; Goldstein et al., 1996; Zilberberg et al., 2001) sensitive to external pH via a histidine in the pore like K2P3 (Lopes et al., 2001) and K2P9 (Rajan et al., 2000). Native K2P1 channels did not play a role in the measures of excitability studied here because they pass a small fraction of hippocampal neuron potassium flux (Lauritzen et al., 2003) and are readily differentiated from time- and voltage-dependent channels like Kv2.1. In contrast to Kv2.1, heterologous overexpression of Kv1.5 channels with SENP2, or mutation of two predicted SUMO conjugation motifs, is reported to have no effect on current magnitude or activation but to shift voltage-dependent steady-state inactivation without a change in its extent (Benson et al., 2007).

Because sumoylation controls transcription factor half-life and nuclear import/export (Seeler and Dejean, 2003), effects on lifespan and trafficking of other membrane proteins (directly or a result of interference with ubiquitin-mediated degradation) should be expected based on observations of the SUMO pathway at the cell surface. Indeed, GluR6 receptors in rat hippocampal neurons are identified as SUMO targets (Martin et al., 2007), and sumoylation of the receptor in response to kainate is found to lower surface levels via increased endocytosis. In contrast, enhanced sumoylation is proposed to impair endocytosis of mutant cardiac TRPM4 channels identified by their association with familial heart block leading to increased surface levels (Kruse et al., 2009).

Broad potential impact for SUMO pathway regulation of Kv2.1

The SUMO pathway has been recognized to choreograph long-lasting responses in the nervous system, such as neuronal plasticity via transcription factor regulation of cell cycle progression, cell death, and synapse formation. Here, we show that SUMO exerts rapid graded control over the excitability of cultured rat hippocampal neurons through modulation of the operation of Kv2.1 channels at the cell surface. The ubiquity of the SUMO pathway and the broad tissue expression and physiological importance of Kv2.1 channels suggest that the regulation of excitability described here for hippocampal neurons may also be observed in the cerebral and cerebellar cortices, olfactory bulb, retina, and cochlea, and beyond the nervous system in the heart, skeletal muscle, pulmonary arteries, and pancreas. Because Kv2.1 channels mediate potassium flux associated with the initiation of neuronal apoptosis (Pal et al., 2003), the SUMO pathway may also influence cellular architecture of the brain and neuropathology via Kv2.1. It seems likely that this pathway linking rapid and long-term responses will have broad impact within and outside the nervous system.

The authors thank D. Araki, V. Bindokas, D. Goldstein, S. Olikara, A. Schilling, D. Thomas, J. Wang, and D. Wolfgeher for intellectual and technical support.

The work was supported by the National Institutes of Health (grant R01NS058505 to S.A.N. Goldstein and grant R01NS056313 to J.D. Marks).

Kenton J. Swartz served as editor.

Submitted: 26 January 2011
Accepted: 4 April 2011

REFERENCES

Abbott, G.W., M.H. Butler, S. Bendahhou, M.C. Dalakas, L.J. Ptacek, and S.A. Goldstein. 2001. MiRP2 forms potassium channels in skeletal muscle with Kv3.4 and is associated with periodic paralysis. *Cell.* 104:217–231. doi:10.1016/S0092-8674(01)00207-0

Benson, M.D., Q.-J. Li, K. Kieckhafer, D. Dudek, M.R. Whorton, R.K. Sunahara, J.A. Iñiguez-Lluhí, and J.R. Martens. 2007. SUMO modification regulates inactivation of the voltage-gated potassium channel Kv1.5. *Proc. Natl. Acad. Sci. USA.* 104:1805–1810. doi:10.1073/pnas.0606702104

Boggio, R., R. Colombo, R.T. Hay, G.F. Draetta, and S. Chiocca. 2004. A mechanism for inhibiting the SUMO pathway. *Mol. Cell.* 16:549–561. doi:10.1016/j.molcel.2004.11.007

Bossis, G., and F. Melchior. 2006. Regulation of SUMOylation by reversible oxidation of SUMO conjugating enzymes. *Mol. Cell.* 21:349–357. doi:10.1016/j.molcel.2005.12.019

Dai, X.Q., J. Kolic, P. Marchi, S. Sipione, and P.E. Macdonald. 2009. SUMOylation regulates Kv2.1 and modulates pancreatic β-cell excitability. *J. Cell Sci.* 122:775–779. doi:10.1242/jcs.036632

Feliciangeli, S., S. Bendahhou, G. Sandoz, P. Gounon, M. Reichold, R. Warth, M. Lazdunski, J. Barhanin, and F. Lesage. 2007. Does sumoylation control K2P1/TWIK1 background K^+ channels? *Cell.* 130:563–569. doi:10.1016/j.cell.2007.06.012

Flavell, S.W., C.W. Cowan, T.-K. Kim, P.L. Greer, Y. Lin, S. Paradis, E.C. Griffith, L.S. Hu, C. Chen, and M.E. Greenberg. 2006. Activity-dependent regulation of MEF2 transcription factors suppresses excitatory synapse number. *Science.* 311:1008–1012. doi:10.1126/science.1122511

Gareau, J.R., and C.D. Lima. 2010. The SUMO pathway: emerging mechanisms that shape specificity, conjugation and recognition. *Nat. Rev. Mol. Cell Biol.* 11:861–871. doi:10.1038/nrm3011

Goldstein, S.A.N., L.A. Price, D.N. Rosenthal, and M.H. Pausch. 1996. ORK1, a potassium-selective leak channel with two pore domains cloned from Drosophila melanogaster by expression in Saccharomyces cerevisiae. *Proc. Natl. Acad. Sci. USA.* 93:13256–13261. doi:10.1073/pnas.93.23.13256

Hay, R.T. 2005. SUMO: a history of modification. *Mol. Cell.* 18:1–12. doi:10.1016/j.molcel.2005.03.012

Jares-Erijman, E.A., and T.M. Jovin. 2003. FRET imaging. *Nat. Biotechnol.* 21:1387–1395. doi:10.1038/nbt896

Kenworthy, A.K. 2001. Imaging protein-protein interactions using fluorescence resonance energy transfer microscopy. *Methods.* 24: 289–296. doi:10.1006/meth.2001.1189

Ketchum, K.A., W.J. Joiner, A.J. Sellers, L.K. Kaczmarek, and S.A.N. Goldstein. 1995. A new family of outwardly rectifying potassium channel proteins with two pore domains in tandem. *Nature.* 376: 690–695. doi:10.1038/376690a0

Knuesel, M., H.T. Cheung, M. Hamady, K.K.B. Barthel, and X. Liu. 2005. A method of mapping protein sumoylation sites by mass spectrometry using a modified small ubiquitin-like modifier 1 (SUMO-1) and a computational program. *Mol. Cell. Proteomics.* 4:1626–1636. doi:10.1074/mcp.T500011-MCP200

Kruse, M., E. Schulze-Bahr, V. Corfield, A. Beckmann, B. Stallmeyer, G. Kurtbay, I. Ohmert, E. Schulze-Bahr, P. Brink, and O. Pongs. 2009. Impaired endocytosis of the ion channel TRPM4 is associated with human progressive familial heart block type I. *J. Clin. Invest.* 119:2737–2744. doi:10.1172/JCI38292

Lauritzen, I., M. Zanzouri, E. Honoré, F. Duprat, M.U. Ehrengruber, M. Lazdunski, and A.J. Patel. 2003. K+-dependent cerebellar granule neuron apoptosis. Role of task leak K+ channels. *J. Biol. Chem.* 278:32068–32076. doi:10.1074/jbc.M302631200

Levitan, I.B. 1994. Modulation of ion channels by protein phosphorylation and dephosphorylation. *Annu. Rev. Physiol.* 56:193–212. doi:10.1146/annurev.ph.56.030194.001205

Levitan, I.B. 2006. Signaling protein complexes associated with neuronal ion channels. *Nat. Neurosci.* 9:305–310. doi:10.1038/nn1647

Li-Smerin, Y., and K.J. Swartz. 1998. Gating modifier toxins reveal a conserved structural motif in voltage-gated Ca2+ and K+ channels. *Proc. Natl. Acad. Sci. USA.* 95:8585–8589. doi:10.1073/pnas.95.15.8585

Lim, S.T., D.E. Antonucci, R.H. Scannevin, and J.S. Trimmer. 2000. A novel targeting signal for proximal clustering of the Kv2.1 K+ channel in hippocampal neurons. *Neuron.* 25:385–397. doi:10.1016/S0896-6273(00)80902-2

Lopes, C.M.B., N. Zilberberg, and S.A.N. Goldstein. 2001. Block of Kcnk3 by protons. Evidence that 2-P-domain potassium channel subunits function as homodimers. *J. Biol. Chem.* 276:24449–24452. doi:10.1074/jbc.C100184200

Marks, J.D., C. Boriboun, and J. Wang. 2005. Mitochondrial nitric oxide mediates decreased vulnerability of hippocampal neurons from immature animals to NMDA. *J. Neurosci.* 25:6561–6575. doi:10.1523/JNEUROSCI.1450-05.2005

Martin, S., A. Nishimune, J.R. Mellor, and J.M. Henley. 2007. SUMOylation regulates kainate-receptor-mediated synaptic transmission. *Nature.* 447:321–325. doi:10.1038/nature05736

Melchior, F., M. Schergaut, and A. Pichler. 2003. SUMO: ligases, isopeptidases and nuclear pores. *Trends Biochem. Sci.* 28:612–618. doi:10.1016/j.tibs.2003.09.002

Misonou, H., D.P. Mohapatra, E.W. Park, V. Leung, D. Zhen, K. Misonou, A.E. Anderson, and J.S. Trimmer. 2004. Regulation of ion channel localization and phosphorylation by neuronal activity. *Nat. Neurosci.* 7:711–718. doi:10.1038/nn1260

Misonou, H., D.P. Mohapatra, M. Menegola, and J.S. Trimmer. 2005. Calcium- and metabolic state-dependent modulation of the voltage-dependent Kv2.1 channel regulates neuronal excitability in response to ischemia. *J. Neurosci.* 25:11184–11193. doi:10.1523/JNEUROSCI.3370-05.2005

Murakoshi, H., and J.S. Trimmer. 1999. Identification of the Kv2.1 K+ channel as a major component of the delayed rectifier K+ current in rat hippocampal neurons. *J. Neurosci.* 19:1728–1735.

O'Connell, K.M.S., R. Loftus, and M.M. Tamkun. 2010. Localization-dependent activity of the Kv2.1 delayed-rectifier K+ channel. *Proc. Natl. Acad. Sci. USA.* 107:12351–12356. doi:10.1073/pnas.1003028107

Pal, S., K.A. Hartnett, J.M. Nerbonne, E.S. Levitan, and E. Aizenman. 2003. Mediation of neuronal apoptosis by Kv2.1-encoded potassium channels. *J. Neurosci.* 23:4798–4802.

Park, K.-S., D.P. Mohapatra, H. Misonou, and J.S. Trimmer. 2006. Graded regulation of the Kv2.1 potassium channel by variable phosphorylation. *Science.* 313:976–979. doi:10.1126/science.1124254

Plant, L.D., P.N. Bowers, Q. Liu, T. Morgan, T.T. Zhang, M.W. State, W. Chen, R.A. Kittles, and S.A.N. Goldstein. 2006. A common cardiac sodium channel variant associated with sudden infant death in African Americans, SCN5A S1103Y. *J. Clin. Invest.* 116:430–435. doi:10.1172/JCI25618

Plant, L.D., S. Olikara, S. Rajan, J. Marks, and S.A.N. Goldstein. 2007. Sumoylation of Kv2.1 controls the excitability of hippocampal neurons. *Biophys. J.* 92:12A.

Plant, L.D., I.S. Dementieva, A. Kollewe, S. Olikara, J.D. Marks, and S.A. Goldstein. 2010. One SUMO is sufficient to silence

the dimeric potassium channel K2P1. *Proc. Natl. Acad. Sci. USA.* 107:10743–10748. doi:10.1073/pnas.1004712107

Rajan, S., E. Wischmeyer, G. Xin Liu, R. Preisig-Müller, J. Daut, A. Karschin, and C. Derst. 2000. TASK-3, a novel tandem pore domain acid-sensitive K+ channel. An extracellular histidine as pH sensor. *J. Biol. Chem.* 275:16650–16657. doi:10.1074/jbc.M000030200

Rajan, S., L.D. Plant, M.L. Rabin, M.H. Butler, and S.A.N. Goldstein. 2005. Sumoylation silences the plasma membrane leak K^+ channel K2P1. *Cell.* 121:37–47. doi:10.1016/j.cell.2005.01.019

Rodriguez, M.S., C. Dargemont, and R.T. Hay. 2001. SUMO-1 conjugation in vivo requires both a consensus modification motif and nuclear targeting. *J. Biol. Chem.* 276:12654–12659. doi:10.1074/jbc.M009476200

Sampson, D.A., M. Wang, and M.J. Matunis. 2001. The small ubiquitin-like modifier-1 (SUMO-1) consensus sequence mediates Ubc9 binding and is essential for SUMO-1 modification. *J. Biol. Chem.* 276:21664–21669. doi:10.1074/jbc.M100006200

Sapetschnig, A., G. Rischitor, H. Braun, A. Doll, M. Schergaut, F. Melchior, and G. Suske. 2002. Transcription factor Sp3 is silenced through SUMO modification by PIAS1. *EMBO J.* 21:5206–5215. doi:10.1093/emboj/cdf510

Seeler, J.-S., and A. Dejean. 2003. Nuclear and unclear functions of SUMO. *Nat. Rev. Mol. Cell Biol.* 4:690–699. doi:10.1038/nrm1200

Sekar, R.B., and A. Periasamy. 2003. Fluorescence resonance energy transfer (FRET) microscopy imaging of live cell protein localizations. *J. Cell Biol.* 160:629–633. doi:10.1083/jcb.200210140

Shalizi, A., B. Gaudillière, Z. Yuan, J. Stegmüller, T. Shirogane, Q. Ge, Y. Tan, B. Schulman, J.W. Harper, and A. Bonni. 2006. A calcium-regulated MEF2 sumoylation switch controls postsynaptic differentiation. *Science.* 311:1012–1017. doi:10.1126/science.1122513

Shen, L., M.H. Tatham, C. Dong, A. Zagórska, J.H. Naismith, and R.T. Hay. 2006. SUMO protease SENP1 induces isomerization of the scissile peptide bond. *Nat. Struct. Mol. Biol.* 13:1069–1077. doi:10.1038/nsmb1172

Talley, E.M., G. Solorzano, Q. Lei, D. Kim, and D.A. Bayliss. 2001. Cns distribution of members of the two-pore-domain (KCNK) potassium channel family. *J. Neurosci.* 21:7491–7505.

Tatham, M.H., E. Jaffray, O.A. Vaughan, J.M.P. Desterro, C.H. Botting, J.H. Naismith, and R.T. Hay. 2001. Polymeric chains of SUMO-2 and SUMO-3 are conjugated to protein substrates by SAE1/SAE2 and Ubc9. *J. Biol. Chem.* 276:35368–35374. doi:10.1074/jbc.M104214200

Uchimura, Y., M. Nakamura, K. Sugasawa, M. Nakao, and H. Saitoh. 2004. Overproduction of eukaryotic SUMO-1- and SUMO-2-conjugated proteins in Escherichia coli. *Anal. Biochem.* 331:204–206.

Ulbrich, M.H., and E.Y. Isacoff. 2007. Subunit counting in membrane-bound proteins. *Nat. Methods.* 4:319–321.

Ulrich, H.D. 2005. Mutual interactions between the SUMO and ubiquitin systems: a plea of no contest. *Trends Cell Biol.* 15:525–532. doi:10.1016/j.tcb.2005.08.002

Ulrich, H.D. 2008. The fast-growing business of SUMO chains. *Mol. Cell.* 32:301–305. doi:10.1016/j.molcel.2008.10.010

Zilberberg, N., N. Ilan, and S.A. Goldstein. 2001. KCNKØ: opening and closing the 2-P-domain potassium leak channel entails "C-type" gating of the outer pore. *Neuron.* 32:635–648. doi:10.1016/S0896-6273(01)00503-7